

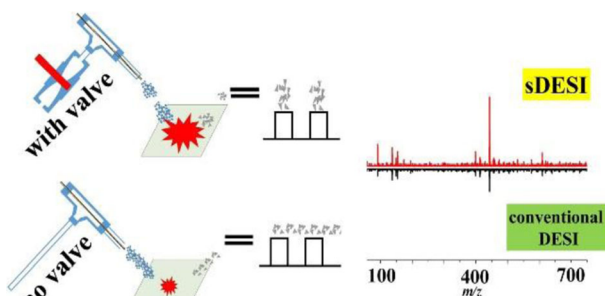
# Enhanced Desorption Electrospray Ionization Mass Spectrometry via Synchronizing Ion Generation and Ion Injection

Zhuanghao Hou,<sup>1</sup> Xingchuang Xiong,<sup>2</sup> Xiang Fang,<sup>2</sup> Guangming Huang<sup>1,3</sup>

<sup>1</sup>Department of Chemistry, School of Chemistry and Materials Science, University of Science and Technology of China (USTC), Hefei, Anhui 230026, People's Republic of China

<sup>2</sup>National Institute of Metrology, Beijing, 100013, People's Republic of China

<sup>3</sup>National Synchrotron Radiation Laboratory, University of Science and Technology of China (USTC), Hefei, Anhui 230026, People's Republic of China



**Abstract.** A modified version of desorption electrospray ionization mass spectrometry was developed for (i) better utilization of analyte ions and (ii) larger sampling area via synchronization the pulsed nebulizer gas with ion injection. To synchronize the sheath gas, gas flow was paused for 50 ms within each cycle, leading to solvent accumulation at the end of emitter tip. That solvent accumulation enlarged the desorption areas. As a result, the amount of analytes

increased. Thus, the improved signal intensity (~2–5-folds for various substrates) was benefit from both better analyte ion utilization and larger desorption areas. Finally, the enhanced signal intensity was confirmed with both garlic homogenate and brain homogenate.

**Keywords:** Mass spectrometer, Synchronized desorption electrospray ionization, Signal enhancement, Ion injection, Ion generation

Received: 18 May 2018/Revised: 29 September 2018/Accepted: 9 October 2018/Published Online: 6 November 2018

## Introduction

Desorption electrospray ionization (DESI) mass spectrometer utilizes high speed solvent droplets for desorption and ionization of samples on a rough surface [1], which has been widely applied for rapid screening [2, 3], polymer characterization [4], forensic identification [5], and biological tissue profiling/imaging [6–10].

In order to further enhance the performance of DESI, intensive efforts have been devoted for complex sample analysis in the last decade, including (i) Introducing tedious sample pre-

treatment such as pre-concentration or imprinting analyte into new substrates (such as nanofiber mat, nanoporous alumina surface, tailored polylactic acid, and polytetrafluoroethylene) to overcome the matrix effect [11–15]. (ii) Apply online or offline derivation [16–19], which would only benefit for targeted analytes. (iii) Using physical treatment such as heating to accelerate sample desorption process [20–22]. However, this method is not suitable for compounds that are heat-instable. Thus, to improve DESI performance in a rapid and universal manner remains challenging.

Another attempt to improve the performance was tested by using large emitter tip and much large solvent flow rate, via much large sampling area (2.5 cm<sup>2</sup>) [23, 24]. While the original goal of that study was to implement large area sampling DESI, it still implies that performance would be enhanced with larger sampling area. However, to achieve large sampling area would require much larger solvent flow rate (6 mL·min<sup>-1</sup>), which would be hard to sustain. Recently, synchronized desorption

**Electronic supplementary material** The online version of this article (<https://doi.org/10.1007/s13361-018-2082-z>) contains supplementary material, which is available to authorized users.

Correspondence to: Xiang Fang; e-mail: fangxiang@nim.ac.cn, Guangming Huang; e-mail: gmhuang@ustc.edu.cn

electrospray ionization (sDESI) has been developed in various ways to enhance DESI performance by precisely controlling the high voltage and sheath gas in time. For example, to minimize “washing effect,” an additional nitrogen shutter gas was introduced to synchronize DESI spray with the movement of the imaging platform for higher spatial resolution [10]. We believe the idea to synchronize DESI spray with MS collection would potentially benefit DESI performance. Since conventional DESI continuously generates ions while the mass spectrometer can only adopt a small amount of the ions (typically ~1–10%, for ion trap MS instrument). Consequently, large amount of ions generated by DESI has not been fully utilized. Previously, we have achieved better sampling efficiency by synchronizing DESI spray plumes with home-built MS instrument [25], with a pulsed potential to precisely control high voltage at millisecond level. We believe with both improvement from (i) better analyte ion efficiency and (ii) larger sampling area due to solvent accumulation, the performance of DESI would be enhanced in a rapid and universal manner. However, the previous set up needed to synchronize the high voltage, the spray plumes, and the MS ion injection, which was quite complicated and could only be achieved on a home-built MS instrument. Until we could control every ion injection events of the commercial MS instrument, it would be impossible to synchronize ion generation and ion capture on widely used benchtop MS.

In this work, a modified sDESI is developed by synchronizing the pulsed gas of DESI with trigger voltage from each ion injection event to achieve better performance. In that way, with a minimal modification of DESI-MS instrument, (including a pinch valve and a DC gate voltage to control sheath gas), synchronization of ion generation and ion capture was achieved on benchtop MS instrument. In addition, larger desorption area for sDESI was discovered than that of conventional DESI, due to solvent accumulation in sDESI emitter during intervals of every sheath gas pulsations. Thus, sampling efficiency was improved (via synchronization) and amount of detected analytes in each measurement was increased (via solvent accumulation), as a result, the performance of sDESI was improved.

## Experimental

### *Materials and Reagents*

Rhodamine B and reserpine were purchased from Sigma-Aldrich Co., Ltd. (United States). Dopamine was purchased from Alfa Aesar Co., Ltd. (Shanghai, China). Acetylcholine and methacholine were purchased from Kuerhuaxue Co., Ltd. (Beijing, China). All chemicals used in this study were of analytically pure grade. Methanol and acetonitrile were bought from J&K Scientific Co., Ltd. (Shanghai, China) in liquid chromatography (LC)-MS quality. Ultrapure water (18.2 M $\Omega$ ) was purified by Milli-Q<sup>®</sup> Reference System (Millipore Corp., USA). 0.4-mm thick polytetrafluorethylene

(PTFE) material was purchased from ShenZhen Anceley Insulated Plastic Material Co., Ltd.

### *Sample Preparation*

The PTFE plates with the diameter of 4 mm were made by a hole puncher. The plates were washed by pure methanol to clean the contaminant before experiments.

To test the performance of sDESI and conventional DESI, 2.5  $\mu$ L of rhodamine B (100 mg L<sup>-1</sup>) was spotted on the glass slides and allowed to dry at room temperature. Subsequently, the glass slides were applied test the synchronized performance states of sDESI. To test the effect of substrates of sDESI and conventional DESI, rhodamine B, reserpine, and dopamine were mixed together with the ratio of (1 mg L<sup>-1</sup>:20 mg L<sup>-1</sup>:50 mg L<sup>-1</sup>). A total of 2.5  $\mu$ L of mixed solution was spotted onto the glass slides (an area of about 100 mm<sup>2</sup>), paper (an area of about 100 mm<sup>2</sup>), PTFE (an area of 12.64 mm<sup>2</sup>), and PTFE (pre-spotted with 2.5  $\mu$ L of brain homogenate, an area of 12.64 mm<sup>2</sup>), respectively.

For real biological sample desorption, the brain and garlic homogenates were made as follows. All animal experiment procedures were approved by the Institutional Animal Care and Use Committee of the University of Science and Technology of China (USTC). The head of an 8-week-old C57 mouse was cut off and the brain was taken out rapidly. The brain was washed by cold distilled water (4 °C) to remove the blood and then removed the water by filter paper. The brain was placed on ice and weight. The brain tissue was diluted with distilled water (with a dilution rate of 1:10), then brain homogenate was obtained by continuous stirring for 40 min by using a stir bar with ice bath. The garlic homogenate was also made similar with brain homogenate. Both brain and garlic homogenates were stored at -20 °C.

To test the performance of sDESI in quantitative analysis, the standard solutions of methacholine in the 0–500 mg L<sup>-1</sup> concentration range with 5.0 mg L<sup>-1</sup> concentration of acetylcholine was deposited on glass slides and paper. Methacholine in the 0–50 mg L<sup>-1</sup> concentration range with 1.0 mg L<sup>-1</sup> concentration of acetylcholine was deposited on PTFE plates. Methacholine in the 0–750 mg L<sup>-1</sup> concentration range with 50 mg L<sup>-1</sup> concentration of acetylcholine was deposited on brain homogenate spots.

### *Synchronized DESI Mass Spectrometry*

All DESI experiments were carried out with a Finnigan LTQ (Thermo Fisher Scientific, CA, USA) mass spectrometer. Main experimental parameters were as follows: spray voltage, 5 kV; capillary voltage, 35 V; capillary temperature, 275 °C; tube lens, 50 V; collision energy, 30 eV; AGC, off; injection time, 100 ms (200 ms for brain and garlic homogenate desorption). The mass-to-charge range analyzed was 50–750, expect for brain homogenate and garlic homogenate desorption (mass-to-charge range of 50–1500).

A homemade sDESI platform was adapted by adding an 8320G142 precise gas flow valve (ASCO Red-Hat, America)

to the conventional DESI source. A solvent spray of water/methanol (10:90, *v/v*, flow rate of 0.75  $\mu\text{L min}^{-1}$ ) was positioned 1.5 mm from the surface at an angle of 62.5°. The surface-to-inlet distance and tip-to-inlet distance were placed to 4 and 0.5 mm, respectively. The nitrogen gas (99.99% purity) pressure of 145 psi was used.

A homemade control panel was designed to provide stable power and response to the synchronized signal. One of the programs was designed to control the sampling procedure of mass spectrometer by adding an adjustable trigger signal and a waiting signal. Another one was programmed to detect the trigger signal and transmit signal to turn on the DESI gas valve.

To capture the spray plume of synchronized DESI and conventional DESI, a smartphone (Smartisan Nut Pro2) was set with 29.97 frames per second of sampling rate. A halogen lamp unit for cold, high-intensity fiber light source (Minebea Co., Ltd., China) was placed behind the DESI source.

### Data Process

Desorption experiment was determined for more than three times to reduce the measurement error. DESI-MS data was evaluation of extracted ion chromatograms of rhodamine B ( $m/z = 443.42$ ), reserpine ( $m/z = 609.25$ ), dopamine ( $m/z = 154.17$ ), acetylcholine ( $m/z = 146.25$ ), and methacholine ( $m/z = 160.25$ ). In order to minimize the variation, all experiments were measured for three times at least ( $n \geq 3$ ) and the data shown in this study was the mean value of five scans for each experiment.

Limits of detection (LODs) of sDESI and conventional DESI were determined in accordance with the calculation equation as follows [26]:

$$\text{LOD} = 3\delta c/S \quad (1)$$

Where  $\delta$  is the standard deviation of the blank samples signal,  $c$  is the minimal concentration signal of the tested components, and  $S$  is the mean signal intensity value of the analytes at the minimal concentration.

The desorption area measurement was carried out by using sodium hydroxide solution (pH = 13) as the DESI solvent and applying pH test paper as a chromogenic plate. HP LaserJet M1005 scanner was used to scan the pH test paper together with a ruler. The image was later measured by using Nano Measurer 1.2 program to obtain the precise size of desorption area of sDESI and conventional DESI.

## Result and Discussion

### The Procedure of Synchronized DESI

Conventional DESI continuously generates charged droplets, which would waste large amount of ions when ion injection of mass spectrometer is closed. For better utilization of analyte ions, an enhanced DESI mass spectrometry method was achieved via synchronizing ion generation with ion acquisition.

A pinch valve was used to control the sheath gas. When ion injection was closed, the pinch valve was turned off to pause the sheath gas. When ion injection was turned on, the pinch valve was triggered on for ion generations (Figure 1a and figure S1). It is worth mentioning that when sheath gas of sDESI was paused, the spray solvent accumulated at the end of emitter tip, leading to much larger desorption area (relative discussion could be found in the later part of the manuscript). With improved ion utilization efficiency and enlarged desorption area, sDESI could provide higher signal intensity over conventional DESI (Figure 1b).

To test the signal enhancement, three different analytes (dopamine, m.w. = 154.2, rhodamine B, m.w. = 443.4, and reserpine, m.w. = 609.3) deposited on paper substrate were subjected to sDESI and conventional DESI, separately. All three compounds were identified with their characteristic fragment ions via collision-induced dissociation (CID) experiments (dopamine with fragment ion of 137.1 in MS/MS, rhodamine B with fragment ions of 427.8/413.8/399.8 in MS/MS, reserpine with fragment ions of 578.3/448.3/397.3 in MS/MS). The signal intensity of all three molecules was found to be improved by using sDESI comparing to conventional DESI (Figure 1b).

To improve sDESI performance, one key issue for this study is to pause the sheath gas when ion injection was turned off. That was accomplished by using a pinch valve, which was triggered on each time the ion injection was turned on. The pinch valve was controlled via a gate voltage (24 V), which was triggered by a feed-back voltage (red arrow in Figure 2a) from the control circuit of the mass spectrometer. However, normally, there would be a delay between the feed-back voltage and ion injection. The delay time (delay 1 in Figure 2a) was found to be different on each individual MS instrument. Thus, to test out principle, and to maximum the synchronization of the ion generation and ion injection, we added another delay time (as delay 2 in Figure 2a) to compensate the delay time (as delay 1 in Figure 2a). The duration of that delay time (delay 2) was tested in the range of 0–200 ms. As data shown in Figure 2b, when delay 2 was applied as 0 ms or > 100 ms, the signal intensity of rhodamine B was extremely low, which indicating that ion generation was not properly matched with ion injection. When applying 50 ms of delay 2, the signal intensity achieved its maximum values. These results suggested that the ion generation was perfectly synchronized with ion injection using correct delay settings, which leading to the improvement of signal of sDESI. Therefore, an optimized delay time was set as 50 ms in the following experiments.

Short videos were recorded to show the differentiation of spray procedure between conventional DESI and synchronized DESI. We captured the spray procedure of conventional DESI and synchronized DESI at the solvent flow rate of 1.0  $\mu\text{L min}^{-1}$  (videos shown in the supporting online material). The conventional DESI was found to be spraying continuously, while the spray plume of synchronized DESI was pulsating under the control of the pinch valve. With the solvent accumulation at the end of the emitter tip, the spray plume of synchronized DESI was denser than that of conventional DESI (shown in fig S7a-b). The

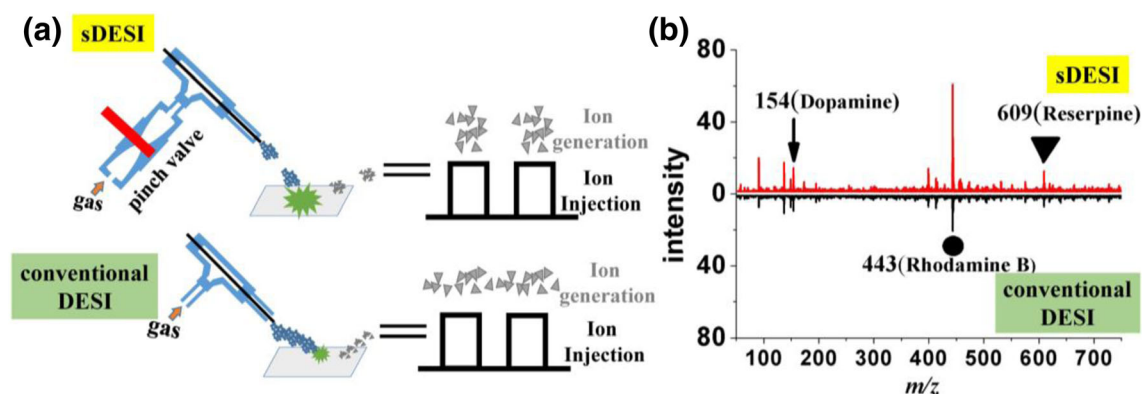


**Figure 1.** (a) Schematic diagram of synchronized desorption electrospray ionization mass spectrometry. A pinch valve was used to synchronize ion generation with ion injection for better utilization of analyte ions. With solvent accumulation at the end of emitter tip, sDESI was triggered by mass spectrometry and led to larger desorption area than conventional DESI. (b) Respective mass spectra of desorption of rhodamine B ( $1 \text{ mg L}^{-1}$ ,  $2.5 \text{ }\mu\text{L}$  on  $100 \text{ mm}^2$ ,  $0.025 \text{ ng mm}^{-2}$ ), reserpine ( $20 \text{ mg L}^{-1}$ ,  $2.5 \text{ }\mu\text{L}$  on  $100 \text{ mm}^2$ ,  $0.5 \text{ ng mm}^{-2}$ ), and dopamine ( $50 \text{ mg L}^{-1}$ ,  $2.5 \text{ }\mu\text{L}$  on  $100 \text{ mm}^2$ ,  $1.25 \text{ ng mm}^{-2}$ ) from paper by using sDESI (red line) and conventional DESI (black line)

videos provided direct evidence of the pulsed spray procedure and enlarged spray plume of our synchronized DESI. With the improvement of the density of spray plume, synchronized DESI achieved the larger desorption area rather than conventional DESI. Consequently, the signal intensity and sensitivity were also slightly enhanced (shown in table S1).

There might be two possible reasons for the signal enhancement, which include (i) the enlarged desorption area of sDESI might pick up more amount of analytes and (ii) the depletion efficiency of sDESI might be increased due to the larger amount of solvent consumption. To confirm which reason is majorly responsible, we characterized both effects for sDESI and conventional DESI.

#### Characterization the Influence of Desorption Area

To measure and compare the desorption area of sDESI and DESI, we used sodium hydroxide solution ( $\text{pH} = 13$ ) as the spray solvent

and applied pH test paper as a chromogenic plate. Spraying sodium hydroxide solution on pH test paper formed a visible spot. The diameter of impact area created by sDESI and conventional DESI are present in Figure 3a (optical image shown in figure S7c). Although the diameter of impact area increased with higher solvent flow rate in both sDESI and conventional DESI, much larger impact area was created by sDESI. At the solvent flow rate of  $0.75 \text{ }\mu\text{L min}^{-1}$ , the diameter of impact spot created by sDESI ( $0.98 \text{ mm}$ ) was 1.6 times larger than that of conventional DESI ( $0.61 \text{ mm}$ ). Similarly, larger impact area was created by sDESI than conventional DESI with different distance between spray tip and sample surface (figure S2). During synchronized procedure, when the ion injection was turned off, the sDESI sheath gas was paused while the spray solvent would accumulate at the end of emitter tip, leading to an enlarged desorption area. In a word, the impact area of sDESI was universally larger than that of conventional DESI due to the accumulation of solvent at the end of the emitter tip.

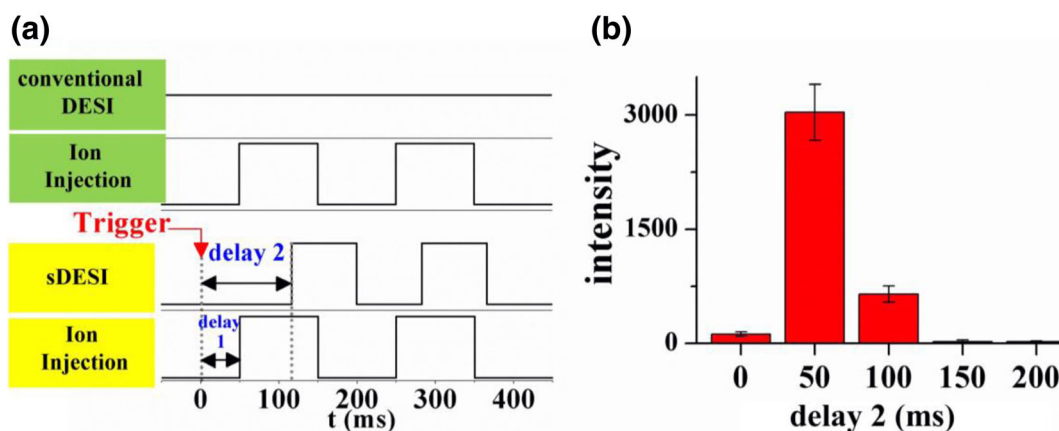


**Figure 2.** (a) Procedure of synchronized sDESI mass spectrometry. Fifty milliseconds ahead of ion injection procedure, a trigger signal was sent out (red arrow) and followed by ion injection for 100 ms. A delay time (black arrow) between catching trigger signal and turning on gas valve was adjustable in order to synchronized DESI spray with ion injection. (b) Signal acquisition of rhodamine B of spotted on glass slides with the concentration of  $5 \text{ ng mm}^{-2}$  ( $100 \text{ mg L}^{-1}$ ,  $2.5 \text{ }\mu\text{L}$  on  $50 \text{ mm}^2$ ) controlled by the delay time 2 of gas valve from 0 to 200 ms

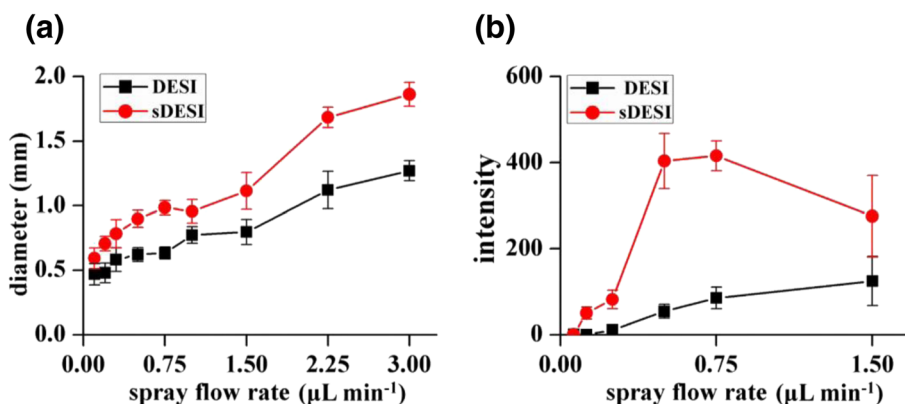


Figure 3. Variation tendency of the diameter of desorption area (a) and the signal intensity of rhodamine B (b) of sDESI and conventional DESI spraying by adjusting the solvent flow rate

With larger impact area, more amount of analyte could be picked up. Glass slides spotted with rhodamine B were submitted to sDESI and conventional DESI to test the the signal enhancement under different solvent flow rates. The data shown in Figure 3b indicated that the signal intensity of rhodamine B obtained by sDESI was higher than that of conventional DESI at different solvent flow rates. Especially in the range of 0.5–0.75  $\mu\text{L min}^{-1}$ , the signal intensity obtained by sDESI was 4.8–7.4-folds higher than that of conventional DESI. However due to large amount of solvent accumulation at the end of the emitter tip under 1.50  $\mu\text{L min}^{-1}$ , the plume of sDESI with too much solvent might prevent the desolvent procedure of analyte which would decrease the ion efficiency. So at such condition, the ion signal intensity was proportional to the desorption area, but still improved.

As a result, with improved ion utilization efficiency and enlarged desorption area, more amount of analyte could be picked up which would be helpful to the enhancement of the signal intensity of sDESI without any sample pre-treatment.

### Characterization the Influence of Depletion Efficiency

To explore the depletion efficiency of sDESI and DESI, we compared the signal intensity of sDESI and conventional DESI under area-unlimited sampling and area-limited sampling mode by adjusting the amount of analyte. As we spotted 2.0  $\mu\text{L}$  of sample solution on the glass slides, the diameter of deposition area (about 5 mm) was much larger than impact area of both sDESI (about 0.98 mm) and conventional DESI (about 0.63 mm). So for both sDESI and conventional DESI, the desorption was under area-unlimited sampling mode. Intensity of sDESI was found to be  $\sim 4$  times higher than that of conventional DESI (data shown in Figure 4a, red histogram). However, when using a 300- $\mu\text{m}$  tip to dip rhodamine B solution on glass slide (deposition was gently repeated to avoid solution spreading), a series of tiny sample spots (about 0.3 mm in diameter) were formed. Under such area-limited sampling mode, the signal intensity obtained by conventional DESI and sDESI was at the similar level (data shown in Figure 4a, blue histogram). The result above suggested that the depletion

efficiency of sDESI might be at the same level with conventional DESI.

To further explore the depletion efficiency, another experiment was carried out. Firstly, we applied conventional DESI and sDESI (first scan) to scan the paper deposited with rhodamine B. Due to larger desorption area, the signal intensity (data shown in Figure 4b with sDESI and DESI label) obtained by sDESI was higher than that of conventional DESI, which was consistent with the result shown in Figure 3b and Figure 4a (red histogram). Secondly, the traces of both sDESI and conventional DESI containing the residues of rhodamine B were submitted to conventional DESI (second scan) to verify the depletion efficiency of the first scan. The signal intensity of second scan (followed with sDESI and conventional DESI) was kept at the similar level (shown in Figure 4b with sDESI/DESI and DESI/DESI label), which implies after first scan, the residues of rhodamine B were at the similar level. That indicated the depletion efficiency of sDESI might be similar to that of conventional DESI.

### Effect of Substrates and Quantification Analysis of sDESI and Conventional DESI

To test the improvement of sDESI on various substrates, four kinds of substrates (glass slides, paper, PTFE, and brain homogenate) spiked with three analytes (dopamine, rhodamine B, and reserpine) were submitted to sDESI and conventional DESI. The ratios of signal intensity and lasting time of sDESI and conventional DESI were presented in Table 1. Among the four substrates, signal intensities were improved for 1.62–5.58-folds with glass slides, paper, and PTFE plates. The signal intensity of molecules was also improved slightly brain homogenates. The respective mass spectrum of all three substrates was shown in Figure 1b, figure S3a–S3c. The lasting time of sDESI was also mildly elevated for 1.0–3.08-folds by comparing to conventional DESI. Three replicate respective spectra of extracted ion chromatography (EIC) of rhodamine B were showed in figure S4a–S4d. In a word, sDESI could reduce effect of substrates obviously and achieve a universal enhancement of both signal intensity and lasting time of various kinds of analytes.

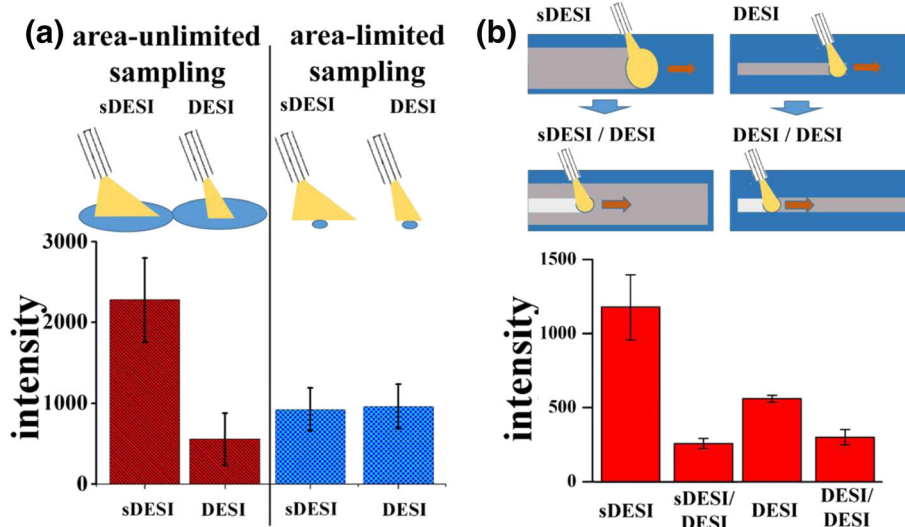


**Figure 4.** (a) The signal intensity of rhodamine B of the larger desorption surface (area-unlimited sampling mode, sampling area of  $\sim 20 \text{ mm}^2$ ,  $12.5 \text{ ng mm}^{-2}$ ) and small desorption surface (area-limited sampling mode, sampling area of  $\sim 0.07 \text{ mm}^2$ ,  $125 \text{ ng mm}^{-2}$ ) obtained by conventional DESI and sDESI. (b) Repeated-scanning of the same line using conventional DESI and sDESI

To verify the quantitative capabilities of sDESI, internal calibration curves were carried out by both sDESI and conventional DESI. Acetylcholine (AC,  $m/z = 146.4$ ) was used as internal standard for methacholine (MAC,  $m/z = 160.4$ ). Methacholine and acetylcholine were identified based on CID experiments (methacholine with fragment ion of 101.1 in MS/MS, acetylcholine with fragment ions of 87.1/60 in MS/MS). The calibration curves showed excellent linear response with correlation coefficient ( $R^2$ ) higher than 0.99 for all compounds tested on various substrates (figure S5) by both sDESI and conventional DESI. In addition, the  $R^2$  in sDESI ( $R^2 > 0.999$ ) was better than that in conventional DESI ( $R^2 > 0.99$ ) on both paper and PTFE. The linear range is more than two orders of magnitude for desorption from glass slides (from 0.063 to  $2.5 \text{ ng mm}^{-2}$ ), paper (from 0.064 to  $2.5 \text{ ng mm}^{-2}$ ), and PTFE plates (from 0.02 to  $1.9 \text{ ng mm}^{-2}$ ). When applying sDESI to complicated biological matrices, such as brain homogenate, the

linear range for methacholine was from 1.2 to  $148 \text{ ng mm}^{-2}$ . Therefore, the proposed method (sDESI) is more accurate and reliable in quantitative analysis compared to conventional DESI.

### The Desorption of Raw Biological Samples by Using sDESI

Finally, sDESI was applied to homogenates of raw biological samples to further verify its enhanced performance for actual sample. Figure 5 shows representative mass spectra of brain homogenate when applying using both sDESI and conventional DESI, respectively. The signal intensity of phospholipids by using sDESI was increased to 1.20–3.08-folds (data shown in Table 2). Series of chemical such as choline ( $m/z = 104$ ), alanine ( $m/z = 132$ ), nrepinephrine ( $m/z = 170$ ), and phosphorylcholine ( $m/z = 184$ ) were also

**Table 1.** Comparison of the Signal Intensity and Lasting Time (sDESI/Conventional DESI) of Rhodamine B, Reserpine, and Dopamine Between sDESI and Conventional DESI from Four Substrates

Species	Substrates	Intensity ratio*	Lasting time ratio**
Rhodamine B	Glass	5.58	1.80
	Paper	2.40	1.68
	PTFE	3.45	2.25
	Brain homogenates	1.62	1.10
Reserpine	Glass	2.56	2.86
	Paper	4.26	2.43
	PTFE	2.83	0.99
	Brain homogenates	1.69	3.08
Dopamine	Glass	3.11	1.29
	Paper	2.32	2.21
	PTFE	3.05	1.80
	Brain homogenates	3.03	1.54

\*Intensity ratio =  $I_{\text{sDESI}}/I_{\text{DESI}}$

\*\*Lasting time ratio =  $t_{\text{sDESI}}/t_{\text{DESI}}$

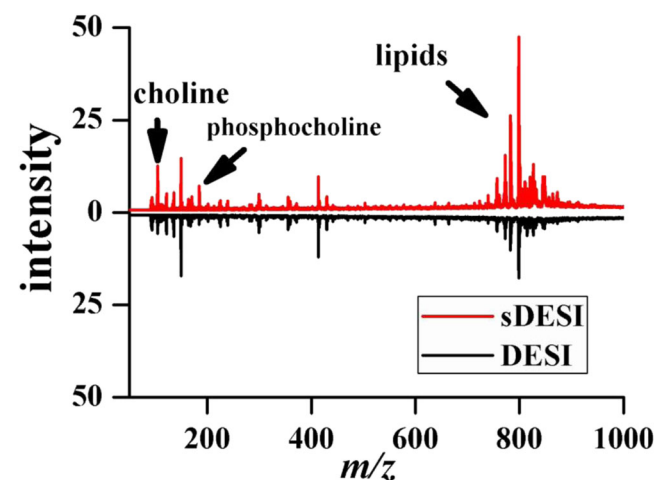


**Figure 5.** Representative mass spectrum of brain homogenates by using sDESI (red line) and conventional DESI (black line)

**Table 2.** Species Detected and Assigned in Positive Ion Mode in Brain Homogenate by Using sDESI and Conventional DESI

Species	<i>m/z</i>	Intensity ratio*	MS/MS
Choline	104	2.41	86/60
Alanine	132	2.05	114/90/86
Norepinephrine	170	1.99	130/84
Phosphorylcholine	184	2.51	136
PC16:0 + Na	518	1.2	459
PC 23:0 + Na	688	0.98	629
PC 32:0	734	1.24	646/478
PC 32:1 + K	770	1.97	711/601/738
PC 34:1 + Na	782.5	3.08	723/601/577
PC 34:1 + K	798.5	3.05	739/615
PC 36:1 + Na	810.5	2.21	751/627
PC 36:1 + K	826.4	2.26	767/643
PC38:4 + Na	832.5	2.09	773/649
PC38:4 + K	848.4	2.45	789

\*Intensity ratio =  $I_{sDESI}/I_{DESI}$

improved when using sDESI. The identified fragment of ions based on CID was listed in Table 2. In addition, sDESI and conventional DESI were also applied to garlic homogenate. The result was consistent with the brain homogenate desorption (respective mass spectra shown in figure S6). Serials of peaks in the mass range of 543 to 1353 with mass shifts of 162 Da were assigned as fructosans ( $(-C_6H_{10}O_5^-)$ , 162 Da), the mass assign result was in accordance with previous reports [27]. The signal intensity of high abundance chemical such as arginine and fructosans in garlic homogenate was found to be improve by 2–3-folds (data shown in table S2). Therefore, for raw biological samples, the improved performance of sDESI was confirmed.

**Conclusion** By synchronizing ion generation and ion injection of DESI, maximum utilization of analyte ions was achieved. Due to the accumulation of solvent at the end of DESI tip, desorption area was also enlarged and more samples were picked up. With such improvement, sDESI enables universal enhancement of signal intensity on various substrates over conventional DESI. However, the performance was also confirmed with raw brain/garlic homogenates. In addition, the synchronizing approach might benefit not only DESI but also other ionization methods (including electrospray ionization), which provide ions continuously.

## Acknowledgements

The authors are grateful for the financial support from the National Natural Science Foundation of China (21775143 and 21475121), National Key Research and Development Program of China (2016YFA0201300), the Innovative Program of Development Foundation of Hefei Center for Physical Science and Technology (2017FXCX003), foundation of MSERC (40-AKYKF1603), and Recruitment Program of Global Expert.

## References

- Takats, Z., Wiseman, J.M., Gologan, B., Cooks, R.G.: Mass spectrometry sampling under ambient conditions with desorption electrospray ionization. *Science*. **306**, 471–473 (2004)
- Leuthold, L.A., Mandscheff, J.F., Fathi, M., Giroud, C., Augsburger, M., Varesio, E., Hopfgartner, G.: Desorption electrospray ionization mass spectrometry: direct toxicological screening and analysis of illicit ecstasy tablets. *Rapid Commun. Mass Spectrom.* **20**, 103–110 (2006)
- Kaupilla, T.J., Wiseman, J.M., Ketola, R.A., Kotiaho, T., Cooks, R.G., Kostianen, R.: Desorption electrospray ionization mass spectrometry for the analysis of pharmaceuticals and metabolites. *Rapid Commun. Mass Spectrom.* **20**, 387–392 (2006)
- Jackson, A.T., Williams, J.P., Scrivens, J.H.: Desorption electrospray ionisation mass spectrometry and tandem mass spectrometry of low molecular weight synthetic polymers. *Rapid Commun. Mass Spectrom.* **20**, 2717–2727 (2006)
- Ifa, D.R., Gumaelius, L.M., Eberlin, L.S., Manicke, N.E., Cooks, R.G.: Forensic analysis of inks by imaging desorption electrospray ionization (DESI) mass spectrometry. *Analyst*. **132**, 461–467 (2007)
- Okutan, S., Hansen, H.S., Janfelt, C.: Cryo-sectioning of mice for whole-body imaging of drugs and metabolites with desorption electrospray ionization mass spectrometry imaging—a simplified approach. *Proteomics*. **16**, 1634–1641 (2016)
- Shariatgorji, M., Strittmatter, N., Nilsson, A., Kallback, P., Alvarsson, A., Zhang, X., Vallianatou, T., Svenningsson, P., Goodwin, R.J.A., Andren, P.E.: Simultaneous imaging of multiple neurotransmitters and neuroactive substances in the brain by desorption electrospray ionization mass spectrometry. *Neuroimage*. **136**, 129–138 (2016)
- Jarmusch, A.K., Alfaro, C.M., Pirro, V., Hattab, E.M., Cohen-Gadol, A.A., Cooks, R.G.: Differential lipid profiles of normal human brain matter and gliomas by positive and negative mode desorption electrospray ionization-mass spectrometry imaging. *PLoS One*. **11**, (2016)
- Jarmusch, A.K., Pirro, V., Baird, Z., Hattab, E.M., Cohen-Gadol, A.A., Cooks, R.G.: Lipid and metabolite profiles of human brain tumors by desorption electrospray ionization-MS. *P. Natl. Acad. Sci. U.S.A.* **113**, 1486–1491 (2016)
- Comi, T.J., Ryu, S.W., Perry, R.H.: Synchronized desorption electrospray ionization mass spectrometry imaging. *Anal. Chem.* **88**, 1169–1175 (2016)
- Sen, A.K., Nayak, R., Darabi, J., Knapp, D.R.: Use of nanoporous alumina surface for desorption electrospray ionization mass spectrometry in proteomic analysis. *Biomed. Microdevices*. **10**, 531–538 (2008)
- Elvir, L., Forest, R., Bianchera, A., Silvestri, M., Bettini, R.: 3D-printed polylactic acid supports for enhanced ionization efficiency in desorption electrospray mass spectrometry analysis of liquid and gel samples. *Talanta*. **155**, 321–328 (2016)
- Sun, X., Miao, Z., Yuan, Z., Harrington, P.d.B., Colla, J., Chen, H.: Coupling of single droplet micro-extraction with desorption electrospray ionization-mass spectrometry. *Int. J. Mass Spectrom.* **301**, 102–108 (2011)
- Thunig, J., Hansen, S.H., Janfelt, C.: Analysis of secondary plant metabolites by indirect desorption electrospray ionization imaging mass spectrometry. *Anal. Chem.* **83**, 3256–3259 (2011)
- Tata, A., Perez, C., Campos, M.L., Bayfield, M.A., Eberlin, M.N., Ifa, D.R.: Imprint desorption electrospray ionization mass spectrometry imaging for monitoring secondary metabolites production during antagonistic interaction of fungi. *Anal. Chem.* **87**, 12298–12304 (2015)
- Cotte-Rodriguez, I., Takats, Z., Talaty, N., Chen, H.W., Cooks, R.G.: Desorption electrospray ionization of explosives on surfaces: sensitivity and selectivity enhancement by reactive desorption electrospray ionization. *Anal. Chem.* **77**, 6755–6764 (2005)
- Eftekhari, M., Ismail, A.I., Zare, R.N.: Isomeric differentiation of polycyclic aromatic hydrocarbons using silver nitrate reactive desorption electrospray ionization mass spectrometry. *Rapid Commun. Mass Spectrom.* **26**, 1985–1992 (2012)
- Green, F.M., Salter, T.L., Gilmore, I.S., Stokes, P., O'Connor, G.: The effect of electrospray solvent composition on desorption electrospray ionisation (DESI) efficiency and spatial resolution. *Analyst*. **135**, 731–737 (2010)

19. Honarvar, E., Venter, A.R.: Ammonium bicarbonate addition improves the detection of proteins by desorption electrospray ionization mass spectrometry. *J. Am. Soc. Mass Spectrom.* **28**, 1109–1117 (2017)
20. Devenport, N.A., Sealey, L.C., Alruways, F.H., Weston, D.J., Reynolds, J.C., Creaser, C.S.: Direct detection of a sulfonate ester genotoxic impurity by atmospheric-pressure thermal desorption-extractive electrospray-mass spectrometry. *Anal. Chem.* **85**, 6224–6227 (2013)
21. Cho, Y.-T., Su, H., Lin, S.-J., Wu, B.-H., Lai, C.-Y., Huang, I.C.: Using thermal desorption electrospray ionization mass spectrometry to rapidly determine antimicrobial preservatives in cosmetics. *Rapid Commun. Mass Spectrom.* **30**, 2315–2322 (2016)
22. Mattarozzi, M., Bianchi, F., Milioli, M., Cavazza, A., Careri, M.: An innovative method based on quick, easy, cheap, effective, rugged, and safe extraction coupled to desorption electrospray ionization-high resolution mass spectrometry for screening the presence of paralytic shellfish toxins in clams. *Talanta*. **147**, 416–421 (2016)
23. Soparawalla, S., Salazar, G.A., Perry, R.H., Nicholas, M., Cooks, R.G.: Pharmaceutical cleaning validation using non-proximate large-area desorption electrospray ionization mass spectrometry. *Rapid Commun. Mass Spectrom.* **23**, 131–137 (2009)
24. Soparawalla, S., Salazar, G.A., Sokol, E., Perry, R.H., Cooks, R.G.: Trace detection of non-uniformly distributed analytes on surfaces using mass transfer and large-area desorption electrospray ionization (DESI) mass spectrometry. *Analyst*. **135**, 1953–1960 (2010)
25. Huang, G., Li, G., Ducan, J., Ouyang, Z., Cooks, R.G.: Synchronized inductive desorption electrospray ionization mass spectrometry. *Angew. Chem. Int. Ed. Engl.* **50**, 2503–2506 (2011)
26. Zhang, T., Zhou, W., Jin, W., Jin, Q., Chen, H.: Direct detection of aromatic amines and observation of intermediates of Schiff-base reactions by reactive desorption electrospray ionization mass spectrometry. *Microchem. J.* **108**, 18–23 (2013)
27. Zhang, H., Chingin, K., Zhu, L., Chen, H.: Molecular characterization of ongoing enzymatic reactions in raw garlic cloves using extractive electrospray ionization mass spectrometry. *Anal. Chem.* **87**, 2878–2883 (2015)